

On the falls of two wheeled vehicles

Andrea Bonci, Sauro Longhi, Emanuele Lorenzoni and Giuseppe Antonio Scala

Abstract—The study and analysis of two-wheeled vehicle's falls and critical situations are difficult tasks to perform due to the rather elaborate dynamics that come into play. However, to prevent such events, it is necessary a good understanding of the conditions that trigger them. To this purpose, suitable tools able to show how the vehicle's parameters may influence its dynamic behavior are required. In the present paper the analysis of the major falls relative to a two-wheeled vehicle is performed by means of dynamics simulations based on the motorcycle model presented by the authors in prior works. The simulations are also discussed in relation to alternative descriptions provided by theoretical instruments reported in the literature and the substantial consistency of the results is shown.

Keywords— Modeling and simulation, Vehicle dynamics, Two-wheeled vehicles.

I. INTRODUCTION

ACCORDING to a recent study commissioned by the European Union [1], every year, on the European roads, 135.000 people are severely injured. Furthermore, looking at the statistics on the Road fatalities in the EU by transport mode, motorcyclists are accounted for 14 % of road deaths. This percentage still represents a number which must be lowered down by taking advantage of all available technologies on active safety devices. Along with pedestrian and cyclists, motorcyclists are the less protected during a crash that may involve a collision between at least one car or represent a single-vehicle accident whose more common causes include speeding, making wide turns, or sliding out due to rider error.

Andrea Bonci is with the Department of Information Engineering, Università Politecnica delle Marche, via Breccie Bianche, 12, 60131, Ancona, ITALY (corresponding author to provide phone: +39-071-2204666; fax: +39-071-2204224; e-mail: a.bonci@univpm.it).

Sauro Longhi is with the Department of Information Engineering, Università Politecnica delle Marche, via Breccie Bianche, 12, 60131, Ancona, ITALY

Emanuele Lorenzoni is a PhD student at the Department of Information Engineering, Università Politecnica delle Marche, via Breccie Bianche, 12, 60131, Ancona, ITALY

Giuseppe Antonio Scala is a Master's degree student at the Department of Information Engineering, Università Politecnica delle Marche, via Breccie Bianche, 12, 60131, Ancona, ITALY.

In recent years much has been done to improve car's active safety devices such as ABS (Antilock Braking Systems), TCS (Traction Control Systems) and ESC (Electronic Stability Control), and the same road is paved for commercial two-wheeled vehicle. By equipping motorcycles with these kinds of devices mostly it reduces the chance for the vehicle to slip out of the way because of adverse road conditions or rider errors.

The key feature of these devices lays in their ability to detect slipping phenomena in advance so that optimal traction can always be maintained and dangerous trim conditions the rider may no longer be able to correct can be avoided.

On the two-wheeled vehicles the slipping phenomena gives rise to complex behaviors of the vehicle involving besides the kinematic, the dynamic, the bending conditions as well as tires characteristics. Indeed, tires' slippage may have different effects on the vehicle depending on the roll angle, the longitudinal speed, the steering angle, and other aspects of the dynamics. In order to control such phenomena, first of all, it is necessary to understand how they occur and then have suitable tools for the analysis of the parameters which influence the vehicle's behavior. To better analyze the complexity of the falls in the case of two-wheeled vehicles, the authors already proposed an analytical model of a motorcycle [2]-[4] where both the longitudinal and lateral dynamics have been coupled and where the effects of the traction and braking torques applied by the rider have been also taken into account. This model allows to simulate the vehicle's falls and standard descriptions given by other instruments proposed in literature [5]-[6], not particularly suitable for the synthesis of safety controllers, will be compared with the model behavior, which instead could be used in a model-based approach for the synthesis of controllers preventing the falls. Moreover, few works have been proposed in the literature addressing the analysis of the falls, in this regard the reader can refer to [7] for an interesting study performed using a well-known multibody simulator.

In this context, the present work proposes the study of the falls occurring to a two-wheeled vehicle with a comparative approach. The falls will be simulated by the analytical tool developed by the authors and then the phenomena will be analyzed by means of the descriptive theoretical instruments given in literature. This will render possible, during the evolution of the fall, to tuning the safety controllers directly on the model's variables rather than by using the theoretical tools which are not suitable for these purposes.

The first attempt for doing this is to analyze and describe all the phases of a typical fall by the model. This is what we

$$y(x) = D \sin\left\{C \tan^{-1}\left\{Bx - E(Bx - \tan^{-1}(Bx))\right\}\right\} \quad (2)$$

where the output $y(x)$ can describe both the longitudinal force and the lateral force introduced by (1) that are functions of the relative input variable x corresponding to the longitudinal slip λ and the lateral slip α (or side slip) respectively. The slip quantity λ is expressed according to the SAE definition as follow:

$$\lambda = -\frac{V_x - V_R}{V_x} \quad (3)$$

where V_x and V_R are respectively the forward velocity of the vehicle and the rolling velocity of the wheel. In the same way, the sideslip angle is defined as:

$$\alpha = \tan^{-1}\left(\frac{V_y}{V_x}\right) \quad (4)$$

where V_y is the wheel's lateral velocity.

The shape of the curve given by (2) is described by several coefficients among which B is the stiffness factor, C is the shape factor, D is the peak value and E is the curvature factor. The tuning of these coefficients allows to match experimental measures performed with any kind of tire on any kind of road surfaces. For a deeper insight into the Magic Formula, its variants and the meaning of the coefficients, the reader can refer to [5],[6]. Moreover, a review on the methods of extracting these coefficients from experimental measures can be found in [9].

In the basic formulation (2) the longitudinal and lateral slips are considered alone or decoupled, i.e. the formula models the longitudinal force when the effect of the lateral force is not present and vice versa. In this condition, it is said that each force is considered in pure slip condition.

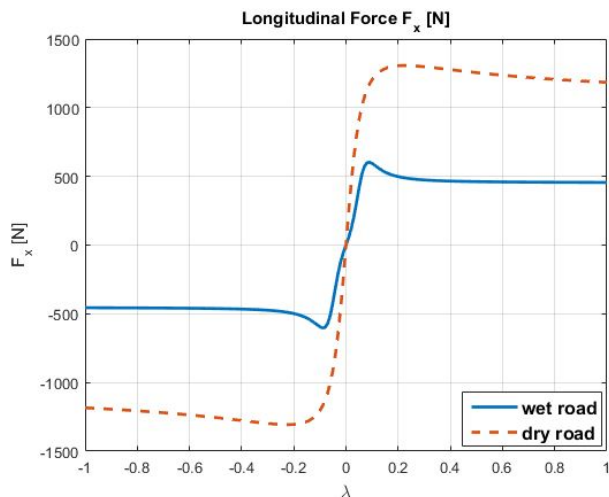


Fig 2 Typical longitudinal forces for different road conditions given by the Magic Formula.

The Figure 2 shows typical profiles for the longitudinal force F_x given by the Magic Formula (2) for dry and wet road surfaces. When the vehicle accelerates, the tire is dragged by a positive force, also known as the driving force or traction force. When the vehicle brakes, the negative force is the braking force. Of course, in wet condition the magnitude of the peaks assumes smaller value than in dry conditions and within the two peaks lays the quasilinear area (grip or traction condition) while the nonlinear part (slipping condition) lays outside.

Moreover, when the motorcycle is in leaning position, the camber angle reaches values beyond the range considered for cars, therefore an equivalent side slip angle is to be considered in the expression (2) for the lateral force in place of α as follow:

$$\alpha_{eq} = \alpha + \frac{k_\phi}{k_\alpha} \phi \quad (5)$$

where ϕ is the wheel camber angle and k_α , k_ϕ are respectively the cornering stiffness and the camber stiffness. Finally, for a motorcycle in cornering conditions the interactions between the longitudinal and the lateral forces cannot be neglected as well in order to model real situations. To this purpose, equation (2) is to be further modified by introducing the following scaling factors, also known as theoretical slips:

$$\begin{cases} \sigma_x = \frac{\lambda}{1 + \lambda} \\ \sigma_y = \frac{\tan \alpha_{eq}}{1 + \lambda} \end{cases} \quad (6)$$

and magnitude:

$$\sigma = \sqrt{\sigma_x^2 + \sigma_y^2} \quad (7)$$

In this way a semi-empirical model of the steady state forces is formed considering the equation (2) for F_x and F_y , wherein the relative slips are replaced with the quantity given by (7):

$$F_{x,y}^{ss} = \frac{\sigma_{x,y}}{\sigma} F_{x,y}(\sigma) \quad (8)$$

The upper script "ss" means that the steady state of the forces is considered. Moreover, their transient behavior should be considered for a realistic situation, indeed these forces arise after a lagging time. To consider this delay, the following relaxation equation for the forces must be introduced:

$$\frac{\zeta_{x,y}}{V_x} \dot{F}_{x,y} + F_{x,y} = \frac{\sigma_{x,y}}{\sigma} F_{x,y}^{ss} \quad (9)$$

where $\zeta_{x,y}$ are the tire relaxation lengths and $F_{x,y}^{ss}$ are given by equation (8).

An alternative graphical representation of the interaction between the forces X and Y is given by the Friction Ellipse. Using this concept, it is possible to determine, for a certain kind of tire, how much traction is left for cornering once the braking force or driving force are accounted for. Figure 3 shows the friction ellipse describing the relationship between X_r and Y_r normalized with respect to the vertical load Z . The subscript “r” stands for the rear wheel and the force Z is the force acting from road to tire along the vertical axis passing from the contact point. Z equals the normal load on that tire. The roll angle is here fixed but in general the ellipse’s profile also depends on it.

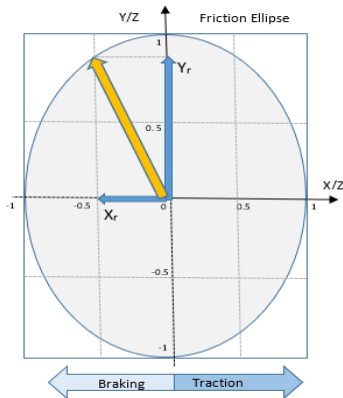


Fig 3 The Friction Ellipse

Figure 3 shows the vector of the total force acting on the tyre and that is the resultant of the longitudinal and the lateral forces. This resultant must lay within the friction ellipse representing the total area available for traction condition. This area varies with the tire size, the suspension geometry, the vehicle attitude and the road conditions.

If X_r is null, the maximum lateral force Y_r is available on the tire, otherwise, if X_r is present, the force Y_r available is reduced and wheel slippage occurs when the longitudinal force applied to the tire exceeds the traction available to that tire (which is dictated by the current friction coefficient and normal load).

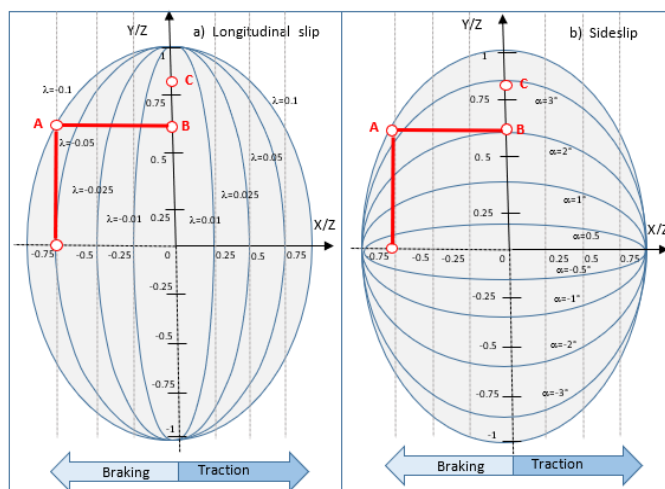


Fig. 4 Friction Ellipses for different values of a) longitudinal slip and b) lateral slips.

Figure 4 details the friction ellipses for a generic tire of a rear traction wheel. Namely, Figure 4 a) shows the curves for constant longitudinal slip λ and Figure 4 b) the ones for constant sideslip α . The points A, B, C highlights the trends of the forces and the corresponding longitudinal and lateral slippage when the vehicle is entering a curve in hard braking. Briefly, at point B the vehicle is running the curve in dynamic equilibrium at a given roll angle, the longitudinal force X on the rear tire is zero because no acceleration or deceleration occurs and the lateral force Y_r in correspondence of the given side slip α keeps the vehicle in balance by counteracting the moments generated by the vertical load Z . If we now assume that the rider starts braking hard, the magnitude of the force X_r increases and the longitudinal slip λ increases as well causing a reduction in the available force Y_r on the tire with consequent increment of the lateral slip α . The dynamics moves from point B to point A while Y_r remains constant. At point B the brake is quickly released thus the braking force decreases accordingly, λ decreases and the tire suddenly regains traction. Namely, if X_r decreases, the lateral force Y_r available on the tire undergoes a sharp increasing and it exceeds the value that was needed previously at point A for the equilibrium. This condition relates to point C and the dynamics has moved from point A to point C at which the vehicle is tilted suddenly upwards. The effect just mentioned by analysing the friction ellipses and rising up between A and C is known as the Highside phenomenon.

In the next sections a brief description of the major fall dynamics will be presented, and their simulations will be shown confirming the preliminary results provided with the friction Ellipses concept.

III. THE TYPICAL DANGEROUS FALLS

A. The Lowside fall

A rider may undergo the low-side fall when the front or rear wheel loses adherence in curve bringing the vehicle to slide away. Typically, this situation occurs at large lean angles and relatively high velocity, moreover it can be fostered by slippery road surface (presence of gravel, oil, water) or improper use of the gas by the rider during the bend. Indeed, the loss of grip of the rear wheel can be experienced at high velocity in a bend as the throttle is abruptly released or opened. Generally, the consequences of the low side fall are not so dramatic unless physical obstacles are present along the way.

B. The Highside fall

The high-side fall is provoked by loss of adherence of the rear wheel in curve due to fast accelerations or hard braking, respectively when coming out of a curve and entering it. With respect to the low-side fall, this one can lead both the rider and the vehicle to ominous situations putting the life of the rider at serious risk. In the first case the phenomenon is excited at excessive speed in curve as the rider starts braking hard to set a better trajectory. This action results in a loss of grip of the

rear wheel which in turn excites a side slippage. This is when the rider suddenly releases the brake to correct the vehicle's attitude, but the rear traction is regained brusquely, the vehicle found itself along a different trajectory and undergoes a rapid straightening due to the high lateral friction force and which may throw away the rider from the saddle. The dynamics is very rapid due to the high moments generated, whose effects are coupled with those caused by the rapid compression and extension of shock absorbers working on the rear wheel and that are strongly excited during this phase.

Modern motorcycles are equipped with active safety systems aiming at controlling the loss of adherence of the traction wheel, hence they help avoid this kind of fall although the probability for the high side to occur cannot be reduced to zero.

IV. SIMULATIONS

In this section the falls' dynamics introduced in prior sections will be simulated and the trends of the major variables involved will be shown. Furthermore, references to the friction circles commonly used in literature will be made which will provide a further qualitative comprehension of the coupling between the frictional forces acting on the traction wheel.

A. The Lowside fall in hard braking and wet conditions

This scenario describes the motorcycle's lowside fall caused by excessive rear braking in curve and wet conditions. The simulation starts with the motorcycle that engages a curve at 40 m/s (144 km/h) with roll angle of about 5-8 Degrees. The trajectory traveled is shown in Figure 5.

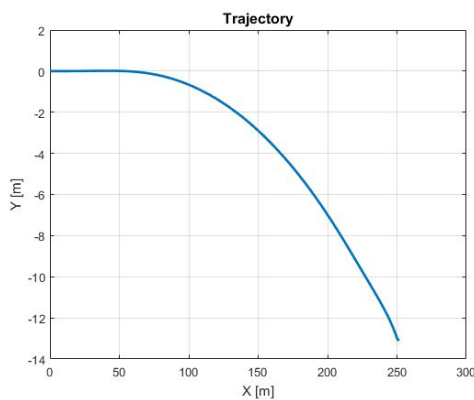


Fig 5 Lowside fall: The Trajectory

The Figure 6 shows the torque T_r applied on the rear wheel in the time window 5-7 seconds. This torque simulates the hard braking applied by the rider.

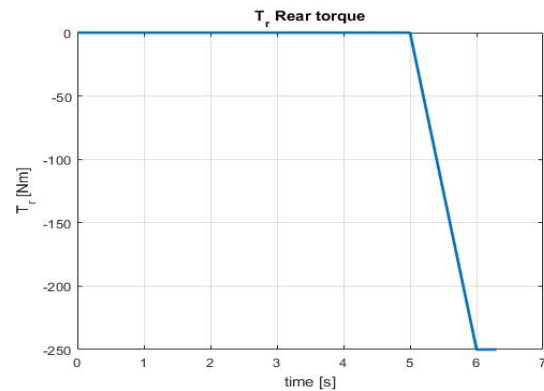


Fig 6 The braking torque applied on the rear wheel

In the same time window, the magnitude of the longitudinal force, i.e. the braking force X_r , shows a growing trend as expected (Figure 10). This braking action leads to the increase in the rear theoretical slip σ_x . Due to the coupling of the forces' dynamics, the slip σ_y increases as well because the friction force available on the tire is reduced in presence of the longitudinal slip. The rear wheel's angular velocity ω_r decreases more strongly with respect to the front wheel's angular velocities ω_f (Figure 7) and the roll angle ϕ drops progressively as shown in Figure 8. In Figure 10 the lateral force Y_r on the rear wheel is shown.

During the braking, the force Y_r starts decreasing and it is never sufficient to keep the motorcycle in balance, as a result the slip quantity of the rear wheel continues to grow as well as the roll angle ϕ . The rider does not even have time to release the brake that at about 6.2 seconds the roll angle has reached such a value that it is impossible for him to regain the correct attitude of the vehicle. Indeed, at around 6.2 seconds the motorcycle reaches an angle ϕ of 90° thus the vehicle falls and the simulation ends.

The results here presented can be compared with those shown in [7] wherein the major falls have been simulated with a well-known multi-body tool. In [7] the Lowside fall in hard braking has been described in case 2) and the trends of the rear tire's forces are shown in Figure 5. In Cossalter's work, the forces's dynamics have been identified by points A-F, while the Figure 10 of our paper shows the same dynamics after time $t = 5$ seconds. Similar trends can be recognized.

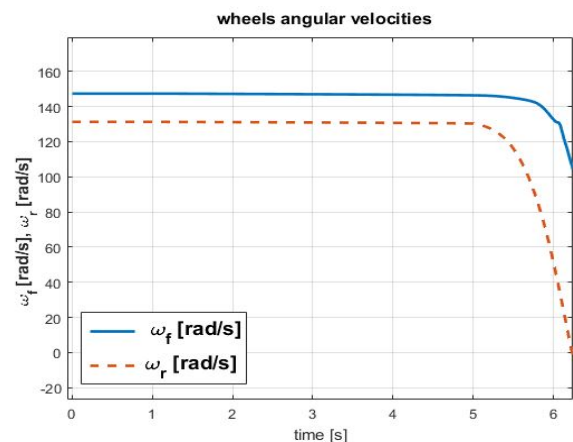


Fig 7 Angular velocities of the front and rear wheels

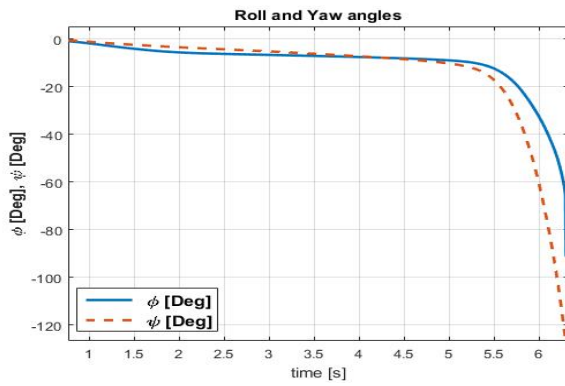


Fig 8 Roll and Yaw angles

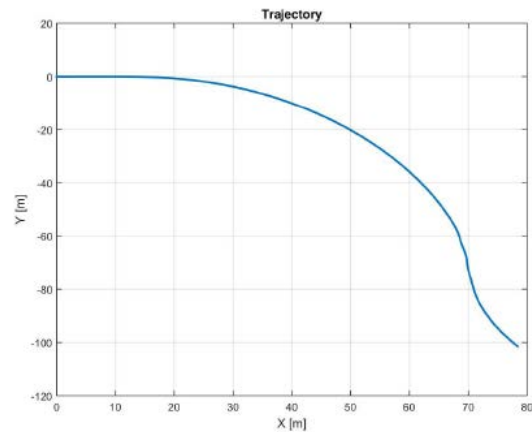


Fig 11 Highside in acceleration: the trajectory

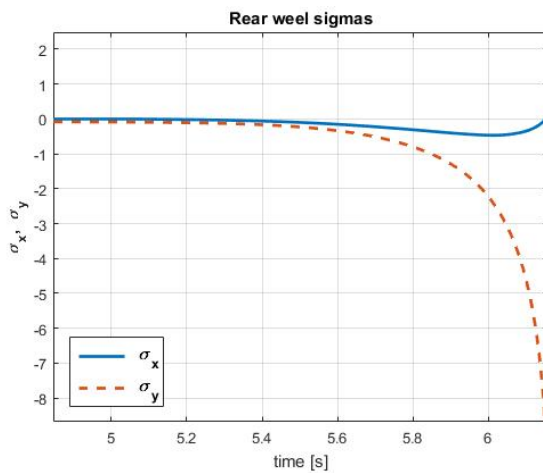


Fig 9 Rear wheel sigmas

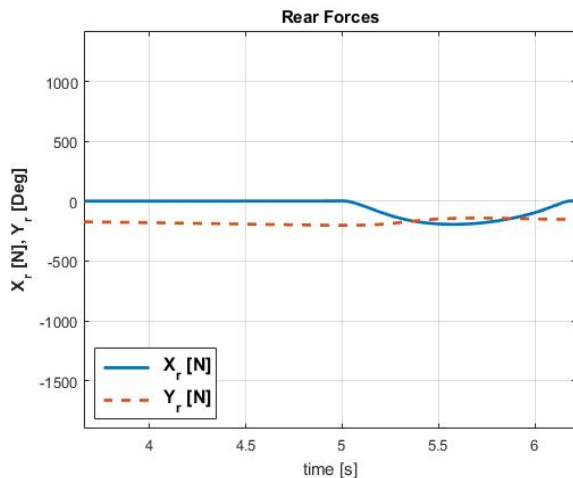


Fig 10 Forces acting on the rear wheel

B. The Highside fall in acceleration and dry condition

This scenario focuses on the case of a motorcycle accelerating hard while coming out of a curve with a steering angle of 1.5° . The Figure 11 shows the trajectory traveled. Note that the figures recalled in the following analysis are put in Appendix for better readability.

As shown in Figure 12, between 2 and 7.5 seconds while the motorcycle is still leaned, the rider opens the throttle, thus T_r increases. Accordingly, the wheels' angular speed increase and the motorcycle accelerates. At about 6 seconds, when the torque reaches 400 Nm, the intensity of the longitudinal force (the driving force) is so high that the rear wheel starts losing adherence: the longitudinal slip increases significantly and as it can be seen in Figure 12, between 6 and 7.5 secs, the rear wheel spin $\dot{\theta}_r$ grows greatly compared to the spin $\dot{\theta}_f$ of the front wheel that moves in pure rolling. This slippage condition agrees with the fact that the theoretical slip σ_x starts diverging from zero significantly. In turn, the increasing in the longitudinal slip affects the lateral dynamic and consequently the theoretical slip σ_y increases more as well. In the same time interval, the lateral force Y_r grows mostly due to the roll angle. At 7.5 seconds (see Figure 12), while experiencing this loss of adherence and large side slip, the rider effectuates a steering rotation to correct the trajectory and he releases suddenly the throttle. As a result, the driving force X_r decreases, and the rear wheel quickly regains traction. Accordingly, σ_x decreases, the wheel speed $\dot{\theta}_r$ and the longitudinal force X_r decrease (see Figure 13). The abrupt traction recovery on the rear wheel results in the Highside phenomenon, i.e. a strong lateral force impulse that at 8 seconds (see Figure 13) pushes up the vehicle violently and triggers a series of oscillations as well which end up dropping the motorcycle.

The dynamics here simulated is qualitatively coherent with the description presented in section II wherein the Highside in hard braking in curve was described by means of generic friction ellipses (figure 4) provided that a positive driving force is considered in place of the braking force and a point A', symmetrical with respect to A is considered in place of point A. It is interesting to observe that the theoretical slips σ_x and σ_y are used in the tire's model for the description of the coupling between the friction forces. Their trends are reported in the graphical results (Fig. 9) and they can be used in the qualitative reasoning in place of the longitudinal slip λ and the sideslip α .

Moreover, one can compare the results presented here with the simulation described in [7] and performed with a multi-body simulator. In [7] the Highside in extreme acceleration in curve

has been described in case 3) and there the trends of the rear tire's forces are shown in Figure 6.

In Cossalter's work, the first stage of the Highside fall can be identified by points A,B,C,D and observing the Figure 13 of our paper, in which the initial phase of the phenomenon occurs in the time window 6-8 seconds, you can say that the two behaviors are quite compatible.

C. The Highside fall in hard braking and dry condition

In this scenario the Highside fall in hard braking is simulated.

The Figure 14 shows the trajectory of the motorcycle approaching a curve at 160 km/h. During the cornering, the excessive rear brake applied by the rider on the rear wheel is simulated with the torque T_r shown in Figure 15. In the same figure are reported the angular velocities of the rear and front wheels, $\dot{\theta}_r$, $\dot{\theta}_f$ and the theoretical slips σ_x , σ_y , relative to the rear wheel. The Figure 16 shows the following quantities: the steering torque τ , the roll angle ϕ , the yaw angle ψ , the longitudinal forces X_r , X_f and the lateral forces Y_r , Y_f . In the time window 0-5 seconds, the braking torque is zero and the vehicle is in cornering equilibrium (Figure 15). Note that this situation refers to the starting condition described qualitatively in section II by means of the friction ellipse concept, Figure 4 a) b), point B. In the same time window, the rear longitudinal force X_r is zero and the rear lateral force Y_r keeps the vehicle in equilibrium (Figure 16). Still at this stage no slip occurs, i.e. σ_x and σ_y are almost zero and constant (Figure 15). Starting from time $t = 5$ seconds up to 6.2 seconds, the rider brakes hence a negative torque T_r is applied to the rear wheel. That means that the magnitude of the braking force X_r starts increasing and in the same time, the rear lateral force Y_r remains substantially constant. At this point the angular velocities of the rear and front wheels $\dot{\theta}_r$ and $\dot{\theta}_f$ start decreasing without significant sliding (Figure 15). Recalling section II and Figure 4 a), b) this is the dynamics moving to the left starting from point B of the friction ellipses.

As the magnitude of the brake torque T_r approaches its maximum, the longitudinal and lateral slips σ_x , σ_y start increasing significantly, then the rear wheel starts losing adherence (Figure 15), in fact the rear angular velocity $\dot{\theta}_r$ decreases more than the front angular velocity $\dot{\theta}_f$ due to the increased rear slip. At time $t = 6.2$ seconds the panicked rider releases quickly the brake (point A of Figure 4 a), b)) in an attempt to correct the lateral slippage and the rear torque T_r quickly decreases to zero accordingly (Figure 15). At this point the rear longitudinal braking force X_r suddenly starts to decrease while the lateral force Y_r significantly increases (Figure 16). This is when the rear wheel regains grip and its angular velocity $\dot{\theta}_r$ starts increasing again (Figure 15). The front angular velocity $\dot{\theta}_f$ increases as well. Starting from time $t = 6.8$ seconds, a series of lateral force impulses Y_r are excited that in turn excite rapid oscillations of the roll and yaw angles (Figure 16). Referring to Figure 11, notice that a steering torque τ has been applied approximatively at time $t = 7.5$ seconds that simulates the rider attempting to regain the

control of the vehicle, which, however, favors the fall. Notice that as the rear slip σ_y approaches to zero at about 7 seconds, the rear tire is in complete adherence and the magnitude of the lateral force Y_r has reached its unbalanced maximum that pushes the vehicle upwards, hence the roll angle increases accordingly. In this situation the rider may be flung from the saddle (Figure 16). This last phase clearly agrees with the dynamics described in section II that moves starting from point A toward point C of Figure 4 a) b) and that refers qualitatively to the Highside in hard braking.

Once the dangerous driving conditions are triggered, the following dynamic evolution is influenced by the rider behavior, the pitch dynamics, the load transfer effects etc. Of course, the lack of these aspects in the modeling affect the accuracy of the simulation if we consider the full dynamics, but that does not invalidate the proposed results, indeed the initial stage of the dynamics under investigation is captured by the model and that represents a factor of major relevance for the design of a control stability system.

References

- [1] European Commission Road Safety (2015). Available at the website http://europa.eu/rapid/press-release_MEMO-17-675_en.htm#_ftnref1A.
A. Bonci, R. De Amicis, S. Longhi, E. Lorenzoni and G. A. Scala. "A motorcycle enhanced model for active safety devices in intelligent transport systems", MESA, Auckland, 2016, pp. 1-6.
- [2] A. Bonci, R. De Amicis, S. Longhi, E. Lorenzoni and G. A. Scala, "Motorcycle's lateral stability issues: Comparison of methods for dynamic modelling of roll angle", 2016 20th International Conference on System Theory, Control and Computing (ICSTCC), Sinaia, Romania, Oct. 13-15, 2016, pp. 607-612.
A. Bonci, R. De Amicis, S. Longhi, E. Lorenzoni, "Comparison of Dynamical Behaviours of Two Motorcycle's Models in the Simulation of Lowside Fall", WSEAS Transactions on Systems and Control, Volume 12, 2017.
- [3] V. Cossalter, Motorcycle dynamics. Lulu.com, 2006.
- [4] H. B. Pacejka, "Tire and Vehicle Dynamics. Butterworth-Heinemann, 2012.
- [5] V. Cossalter, A. Bellati, V. Cafaggi, "Exploratory study of the dynamic behaviour of motorcycle-rider during incipient fall events", In Proceeding of 19th International Technical Conference on the Enhanced Safety of Vehicles Conference (ESV). Washington, D.C. V. (2005)
- [6] H. Dugoff, P. Fancher, L. Segel, "Tire performance characteristics affecting vehicle response to steering and braking control inputs" Ed. by Michigan Highway Safety Research Institute, 1969.
- [7] A. Vijay Alagappan, K. V. Narasimha Rao and R. Krishna Kumar, "A comparison of various algorithms to extract Magic Formula tyre model coefficients for vehicle dynamics simulations: International journal of vehicle mechanics and mobility", 53:2, 154-178, DOI: 10.1080/00423114.2014.984727

APPENDIX

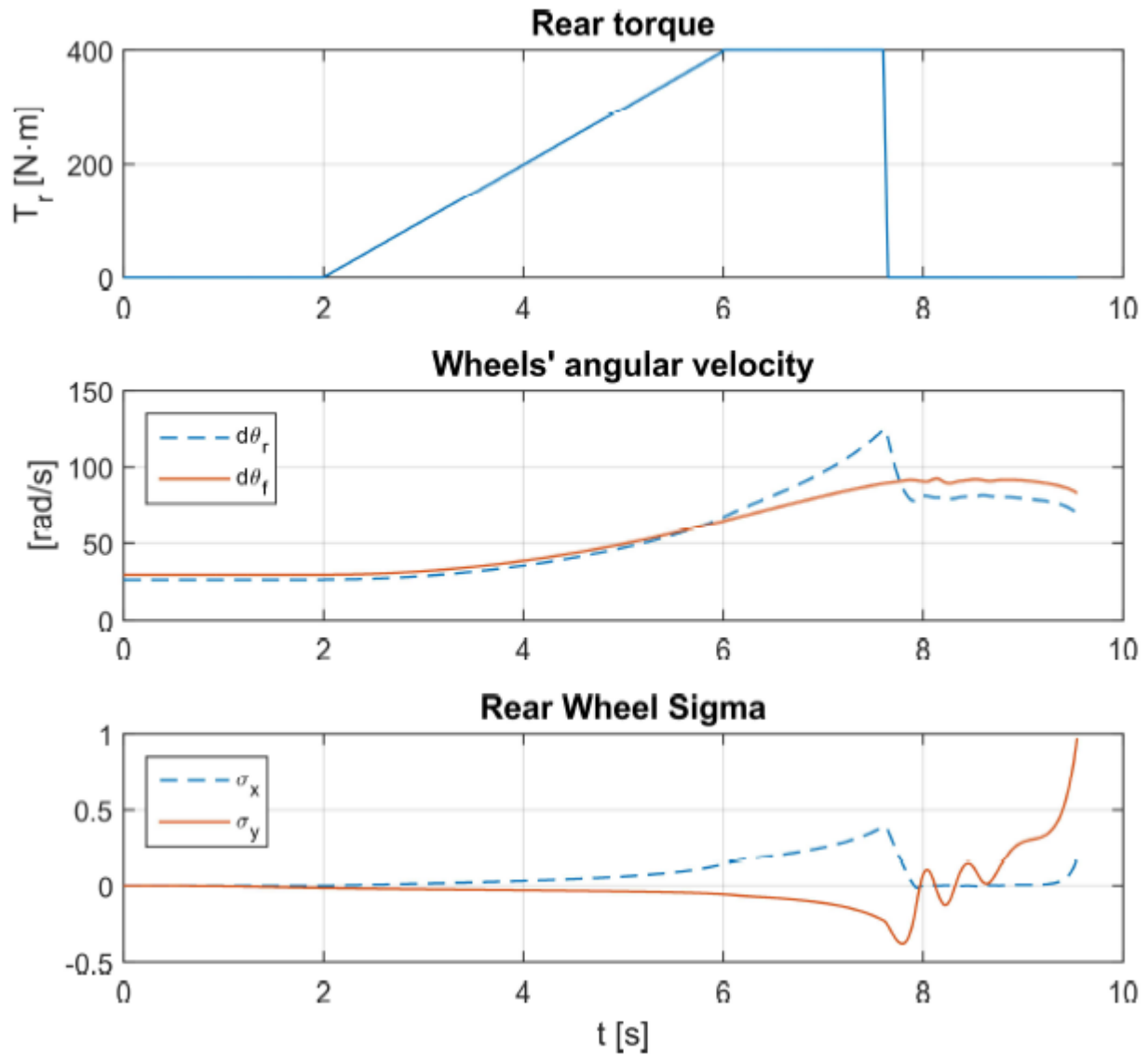


Fig 12 Highside fall in acceleration: Torque applied on the rear wheel, angular velocities of the wheels and rear theoretical slips

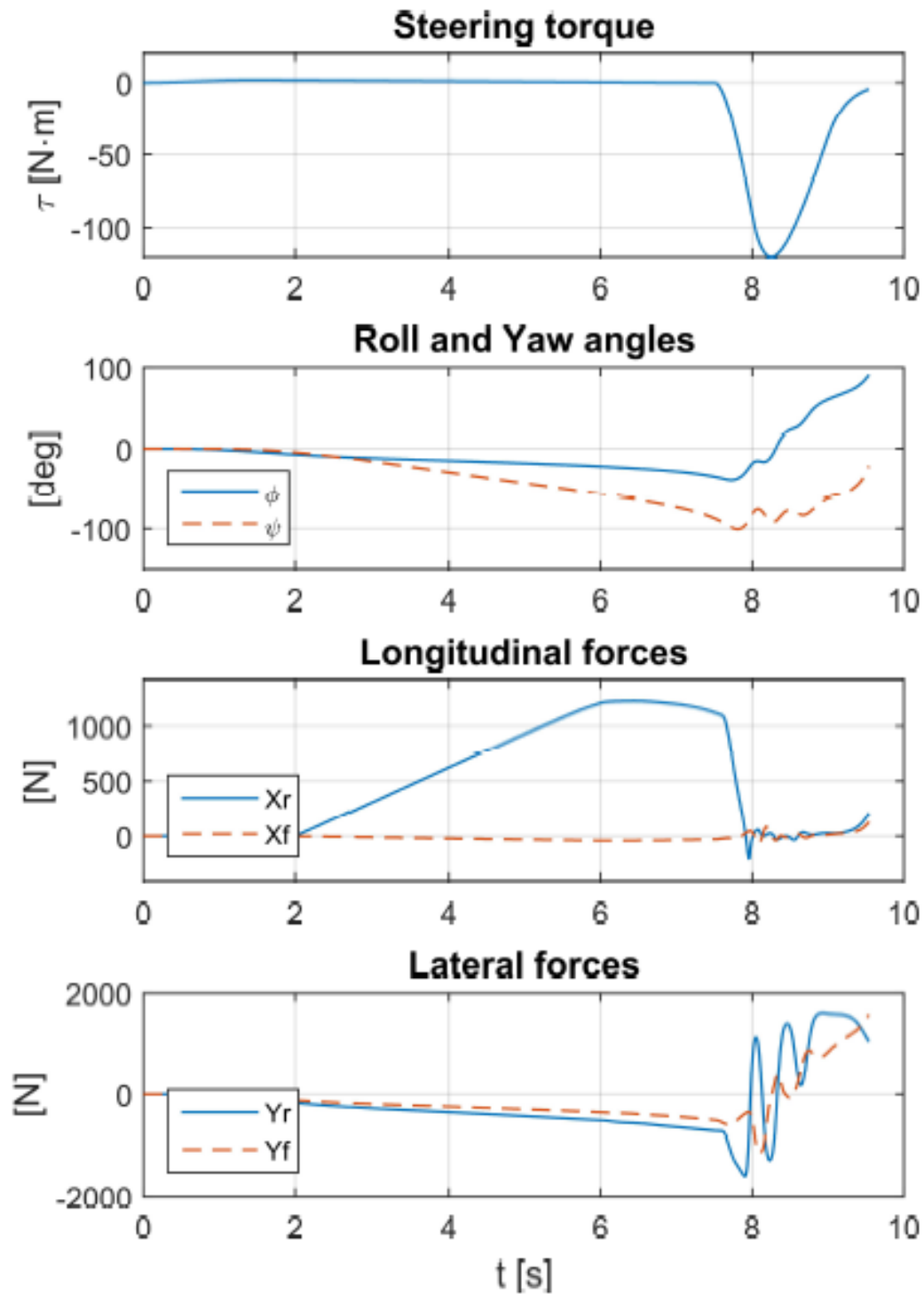


Fig 13 Highside fall in acceleration: The steering torque, roll angle, yaw angle and the friction forces acting on the front and rear wheels

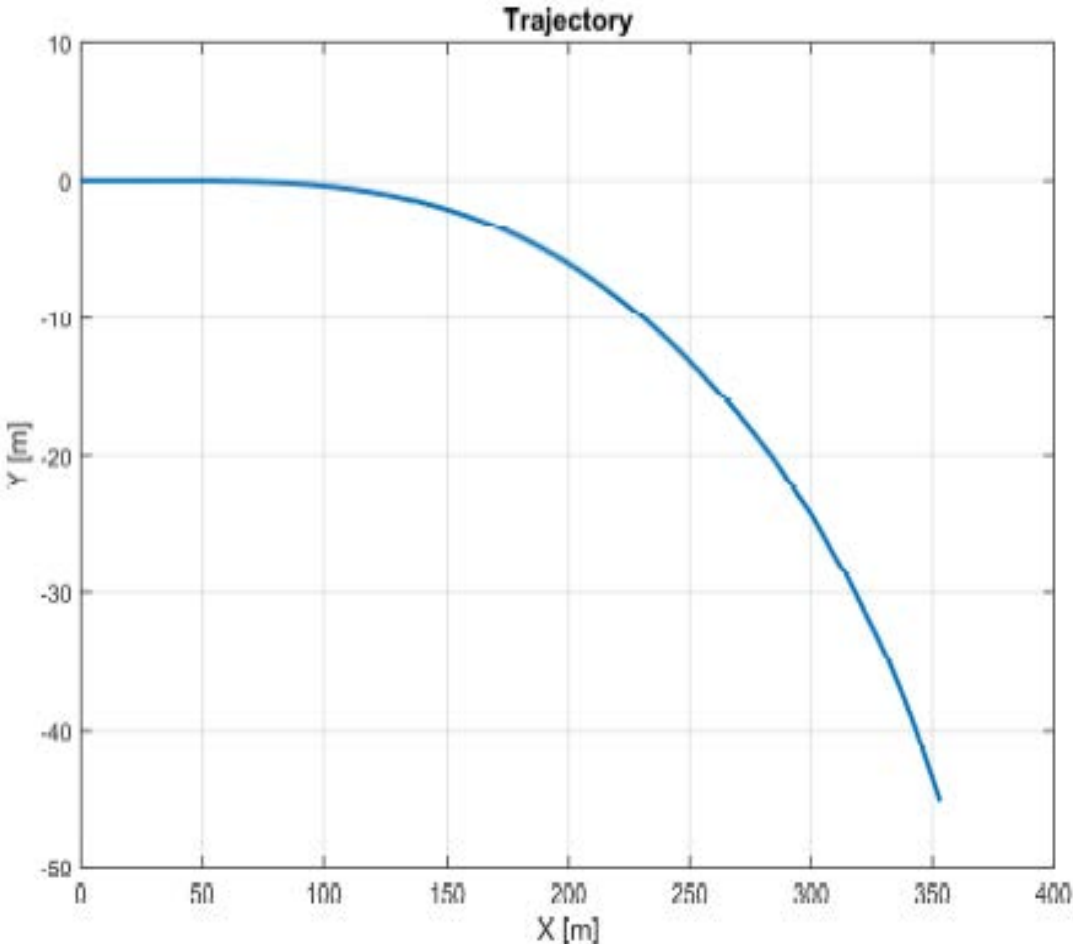


Fig 14 Highside fall in hard braking: the trajectory

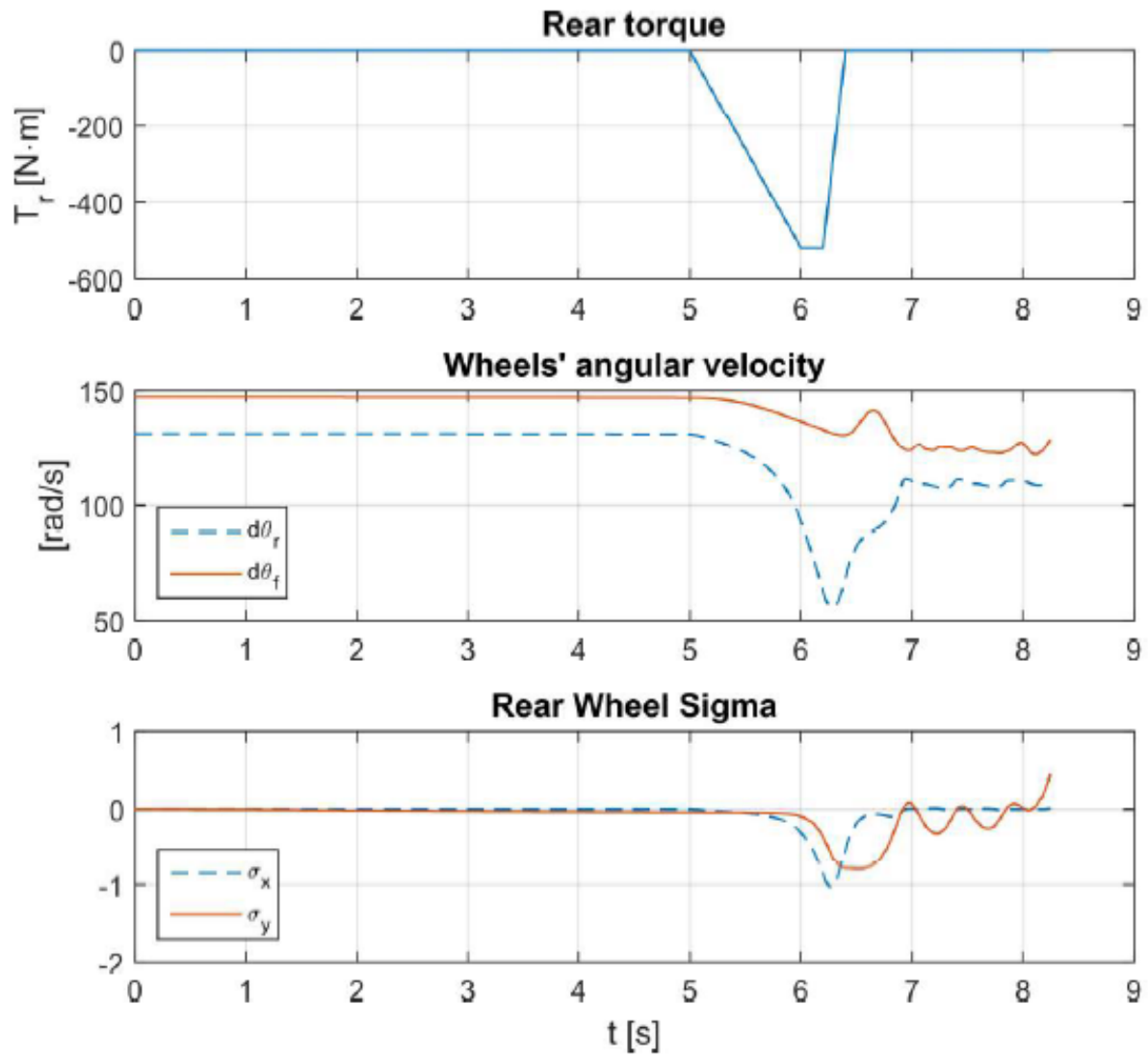


Fig 15 Highside fall in hard braking: The torque applied on the rear wheel, the angular velocities of the wheels and theoretical slips relative to the rear wheel

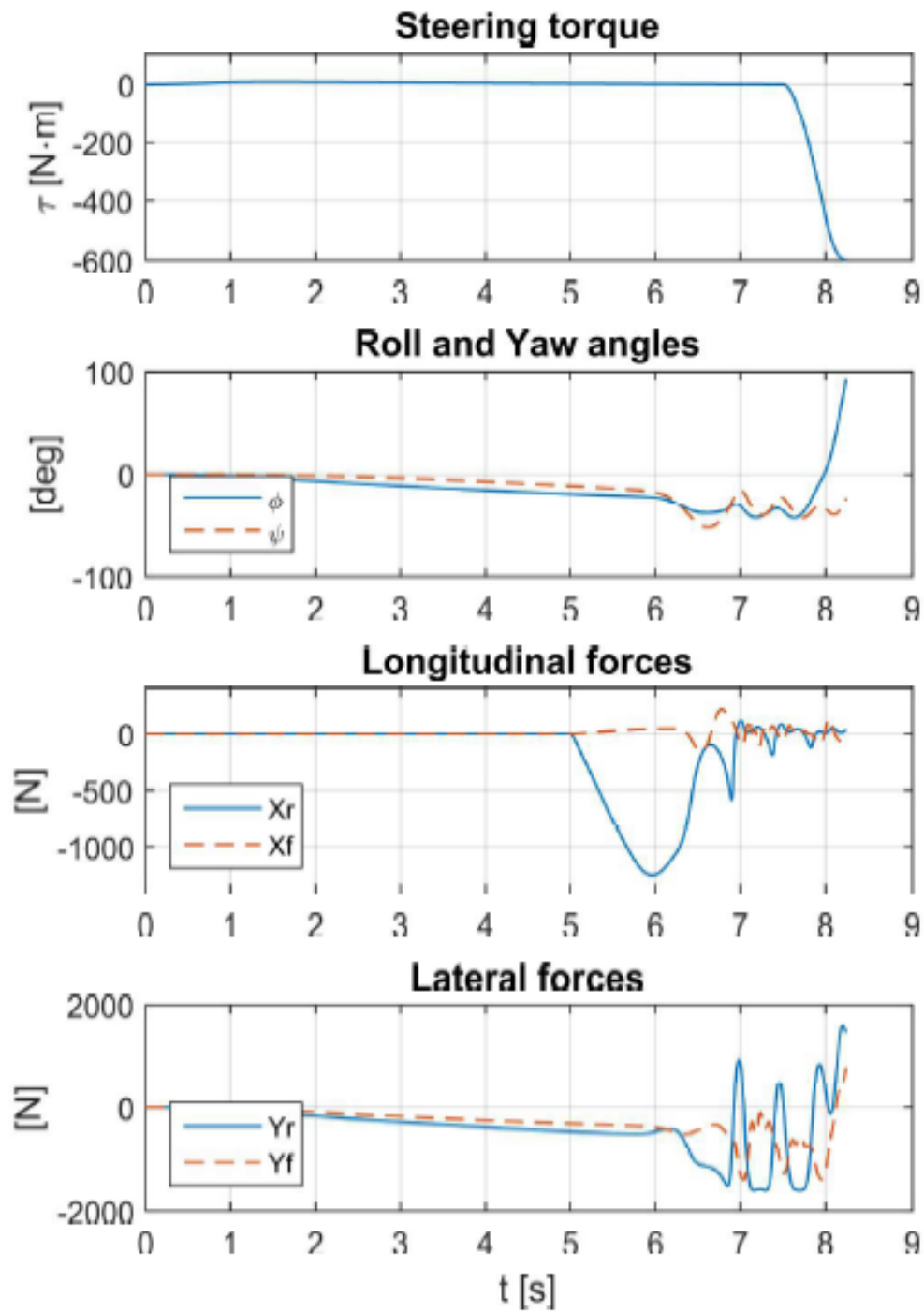


Fig 16 Highside fall in hard braking: Steering torque, roll and yaw angles, forces acting on the traction wheel